

Precision spectroscopy with reactor antineutrinos

Patrick Huber* and Thomas Schwetz†

Physik-Department, Technische Universität München, James-Frank-Strasse, D-85748 Garching, Germany

(Received 19 July 2004; published 17 September 2004)

In this work we present an accurate parameterization of the antineutrino flux produced by the isotopes ^{235}U , ^{239}Pu , and ^{241}Pu in nuclear reactors. We determine the coefficients of this parameterization, as well as their covariance matrix, by performing a fit to spectra inferred from experimentally measured beta spectra. Subsequently we show that flux shape uncertainties play only a minor role in the KamLAND experiment, however, we find that future reactor-neutrino experiments to measure the mixing angle θ_{13} are sensitive to the fine details of the reactor-neutrino spectra. Finally, we investigate the possibility to determine the isotopic composition in nuclear reactors through an antineutrino measurement. We find that with a three month exposure of a 1 ton detector the isotope fractions and the thermal reactor power can be determined at a few percent accuracy, which may open the possibility of an application for safeguard or nonproliferation objectives.

DOI: 10.1103/PhysRevD.70.053011

PACS numbers: 14.60.Pq, 13.15.+g, 28.41.Te

I INTRODUCTION

Experiments at nuclear reactors have a long tradition in neutrino physics. Starting from the experimental discovery of the neutrino at the legendary Cowan-Reines experiment [1], many measurements at nuclear power plants have provided valuable information about neutrinos. For example, the results of the Gösgen [2], Bugey [3], Palo Verde [4], and CHOOZ [5] experiments have led to stringent limits on electron antineutrino disappearance. Reactor-neutrino experiments have become very prominent again due to the outstanding results of the KamLAND experiment [6,7]. For a review on reactor-neutrino experiments, see Ref. [8]. Recently the possibility to determine the last unknown lepton mixing angle θ_{13} by a reactor-neutrino experiment with a near and far detector is actively investigated (see Ref. [9] and references therein). Building on the experience gathered in oscillation experiments ideas of “applied neutrino physics” appeared [10–12]: A detector close to a nuclear reactor could be used for reactor monitoring, either for improving the reliability of operation of power reactors or as a method to accomplish certain safeguard requirements in the context of international treaties for arms control and nonproliferation of weapons of mass destruction.

The standard detection process for reactor neutrinos is inverse beta decay:

$$\bar{\nu}_e + p \rightarrow e^+ + n. \quad (1)$$

The cross section $\sigma(E_\nu)$ for this process is very well known [13], at an accuracy better than 1%. Per fission roughly six electron antineutrinos are produced (see, e.g., Ref. [8]), with energies peaked around 1 MeV. However, for inverse beta decay only neutrinos with energies above

the threshold of 1.8 MeV are relevant. In nuclear reactors electron antineutrinos in that energy range are produced dominantly by the beta decay of the fission products from the four isotopes $\ell = ^{235}\text{U}, ^{239}\text{Pu}, ^{238}\text{U}, ^{241}\text{Pu}$.¹ We denote the flux from the isotope ℓ by $\phi_\ell(E_\nu)$ in units of antineutrinos per fission and MeV. In Table I the total number of $\bar{\nu}_e$ per fission above 1.8 MeV is given for ^{235}U , ^{239}Pu , ^{241}Pu , and ^{238}U .

Accurate information on the antineutrino flux from ^{235}U , ^{239}Pu , and ^{241}Pu can be obtained by the measurement of the beta spectra from the exposure of these isotopes to thermal neutrons [16–18]. Subsequently these beta spectra have to be converted into antineutrino spectra, taking into account the large number of beta branches involved. These spectra are in excellent agreement with the direct observation of the antineutrino spectrum at the Bugey [19] and Rovno [14] reactors. The errors on these fluxes are at the level of a few percent. Since modern reactor-neutrino experiments aim at precisions at this level, a proper treatment of the flux-uncertainties becomes necessary. For ^{238}U , which does only undergo fast neutron fission, no similar measurements exist, and one has to rely on theoretical calculations [20,21].

In absence of neutrino oscillations the number of positron events for a measurement time T in a given positron energy bin i can be calculated by

$$N_i = \frac{n_p T}{4\pi L^2} \sum_\ell N_\ell^{\text{fis}} \int dE_\nu \sigma(E_\nu) \phi_\ell(E_\nu) R_i(E_\nu). \quad (2)$$

¹The next to leading contributions come from the isotopes ^{240}Pu and ^{242}Pu and are of the order 0.1% or less [8]. Further subleading effects are the beta decay of ^{235}U , ^{239}Np , ^{237}U (produced by radiative neutron capture), and corrections to the spectra from fission fragments due to neutron absorption by these fragments [14]. These effects are relevant for the low energy part of the antineutrino spectrum $E_\nu \lesssim 2$ MeV and will be neglected in the following. See, also, Ref. [15].

*Email: phuber@ph.tum.de

†Email: schwetz@ph.tum.de

TABLE I. Total number of $\bar{\nu}_e$ per fission above 1.8 MeV (see Section III for details) and energy release per fission (reproduced from Table two of Ref. [5]) for the isotopes relevant in nuclear reactors.

ℓ	N_ℓ^ν	E_ℓ [MeV]
^{235}U	$1.92(1 \pm 0.019)$	201.7 ± 0.6
^{238}U	$2.38(1 \pm 0.020)$	205.0 ± 0.9
^{239}Pu	$1.45(1 \pm 0.021)$	210.0 ± 0.9
^{241}Pu	$1.83(1 \pm 0.019)$	212.4 ± 1.0

Here n_p is the number of protons in the detector, L is the distance between reactor core and detector, and $R_i(E_\nu)$ is the detector response function for the bin i (including energy resolution and efficiencies). If the initial composition of the reactor fuel is known, the number of fissions per second N_ℓ^{fis} of each isotope ℓ can be calculated accurately (better than 1% [8]) at each burn-up stage by core simulation codes. The thermal power output P of the reactor is given by $P = \sum_\ell N_\ell^{\text{fis}} E_\ell$, where E_ℓ is the energy release per fission for the isotope ℓ , see Table I. Since the errors on E_ℓ are less than 0.5% we will neglect in the following the uncertainty induced by them. Defining the relative contribution of the element ℓ to the total power² f_ℓ , the N_ℓ^{fis} can be expressed by P and Eq. (2) becomes

$$N_i = \frac{n_p T}{4\pi L^2} P \sum_\ell \frac{f_\ell}{E_\ell} \int dE_\nu \sigma(E_\nu) \phi_\ell(E_\nu) R_i(E_\nu)$$

with $f_\ell \equiv \frac{N_\ell^{\text{fis}} E_\ell}{P}$. (3)

The aim of the present work is to consider various aspects of reactor-neutrino spectroscopy, with a main emphasis on issues related to the emitted antineutrino flux. First, in Section II we present a phenomenological parameterization for the antineutrino fluxes ϕ_ℓ based on a polynomial of order 5. We show that in many situations existing parameterizations [22] are not accurate enough to describe the reactor-neutrino spectrum at the required level of precision. In addition, in Section III we give a detailed consideration of the errors associated to the reactor antineutrino spectrum and provide them in a suitable form for implementation in data analyses. In the following we consider the implications of uncertainties of various quantities appearing in Eq. (3) for several experimental configurations. In Section IV we discuss the impact of errors on P , f_ℓ , and ϕ_ℓ for the KamLAND experiment, whereas in Section V we discuss the rele-

vance of our new parameterization of ϕ_ℓ and its errors for future reactor experiments to measure θ_{13} . In Section VI we consider the potential of an antineutrino detector close to a reactor: In Section VIA we discuss the improvement on the flux-uncertainties from a near detector, and in Section VIB we investigate the possibility of reactor monitoring by using the antineutrino measurement. In contrast to previous studies [10–12] we employ full spectral information, which allows the determination of the isotopic content of a reactor, i.e., the fractions f_ℓ , as well as the reactor power P without any external information. We conclude in Section VII.

II. A PARAMETERIZATION FOR THE REACTOR ANTI-NEUTRINO FLUX

In Refs. [16,17] antineutrino spectra from the fission products of ^{235}U , ^{239}Pu , and ^{241}Pu are determined by converting the precisely measured associated beta spectra. In this section we propose a phenomenological parameterization for the reactor antineutrino flux, based on these measurements. Similar as in Ref. [22] we parameterize the spectrum of a given element using a polynomial:

$$\phi_\ell(E_\nu) = \exp\left(\sum_{k=1}^{K_\ell} a_{k\ell} E_\nu^{k-1}\right). \quad (4)$$

The coefficients $a_{k\ell}$ are determined by a fit to the data of Refs. [16,17]. To this aim we minimize the following χ^2 -function:

$$\chi^2 = \sum_{i,j} D_i S_{ij}^{-1} D_j \quad \text{with } D_i \equiv \sum_{k=1}^{K_\ell} a_{k\ell} (E_\nu^{(i)})^{k-1} - \ln \phi_\ell^{(i)}, \quad (5)$$

where $E_\nu^{(i)}$ and $\phi_\ell^{(i)} \equiv \phi_\ell(E_\nu^{(i)})$ are the values of the neutrino energy and the corresponding antineutrino flux, respectively, provided in the tables of Refs. [16,17] for values of the neutrino energy E_ν ranging from 1.5 to 9.5 MeV in steps of 0.25 MeV. Since we are fitting the logarithm of the flux the covariance matrix S_{ij} contains relative errors of the $\phi_\ell^{(i)}$. For the diagonal elements S_{ii} we take the errors as given in the tables of Refs. [16,17] (converted from 90% CL to 1σ and squared), which contain the statistical error from the beta spectrum measurement, a systematic error on the overall calibration, and a systematic error from the conversion from beta to antineutrino spectrum. The off-diagonal elements are obtained from the error on the absolute calibration, which is taken as fully correlated: $S_{ij} = \sigma_i^{\text{cal}} \sigma_j^{\text{cal}}$ for $i \neq j$. The errors σ_i^{cal} are given at two calibration energies for each isotope in Refs. [16–18], and we interpolate linearly between these reference points. Note that this procedure

²The power fractions f_ℓ must not be confused with the relative fission contributions $f_\ell^{\text{fis}} \equiv N_\ell^{\text{fis}} / \sum_\ell N_\ell^{\text{fis}}$. In this case one would obtain $N_\ell^{\text{fis}} = f_\ell^{\text{fis}} P / \langle E \rangle$, where the mean energy per fission is given by $\langle E \rangle = \sum_\ell f_\ell^{\text{fis}} E_\ell$.

TABLE II. Coefficients of the polynomial of order 2. For ^{235}U , ^{239}Pu , ^{241}Pu the numbers are obtained from a fit to the data from Refs. [16,17], for ^{238}U we reproduce the values given in Ref. [22].

ℓ	$a_{1\ell}$	$a_{2\ell}$	$a_{3\ell}$
^{235}U	0.904	-0.184	-0.0878
^{239}U	1.162	-0.392	-0.0790
^{241}Pu	0.852	-0.126	-0.1037
^{238}U	0.976	-0.162	-0.0790

assumes that the systematical errors from the conversion from beta to antineutrino spectrum are completely uncorrelated between different energies.

First we have performed a fit of a polynomial of second order ($K_\ell = 3$). The resulting coefficients $a_{k\ell}$ are given in Table II, and are in reasonable agreement with the ones obtained in Ref. [22] (some deviations appear for ^{241}Pu). However, we find that the quality of this three parameter fit is very bad for all three isotopes (the χ^2 is given in Fig. 1 in the following). We conclude that at the level of precision provided by the errors the data cannot be described with sufficient accuracy by the polynomial of order 2. We have checked that a reasonable fit is obtained

for all three elements only by going up to a polynomial of order 5, corresponding to $K_\ell = 6$ parameters. The best-fit coefficients $a_{k\ell}$ are given in Table III, and the corresponding antineutrino spectra are available in computer readable format at the web-page Ref. [23].

Our fit is illustrated in Fig. 1, where we show the resulting spectra for the three and six parameter fits in comparison to the data. Large differences between the three and six parameter fit are visible by eye only for the high energy region, where the spectra are very small and errors are large. However, comparing the corresponding χ^2 -values $\chi^2_{(3)}$ and $\chi^2_{(6)}$ given in the figure it is obvious that the six parameters are necessary to obtain a reasonable goodness-of-fit. In the lower panels we show the residuals of the fit, i.e., for each data point i we plot $(\phi_{\text{data}}^{(i)} - \phi_{\text{fit}}^{(i)})/\sigma_i$, where the error is obtained from the covariance matrix S by $\sigma_i = \phi_{\text{data}}^{(i)} \sqrt{S_{ii}}$. Note that because of correlations between the $\phi_{\text{data}}^{(i)}$ these residuals do not add up to the total χ^2 . For ^{235}U the three parameter fit shows rather large residuals over the full energy range. Since this isotope gives the main contribution to the reactor antineutrino flux it is very important to model its neutrino spectrum correctly. Let us note that we exclude six data points at high neutrino energies from the fit. The change in the spectral shape around 8 MeV [16] cannot be fitted

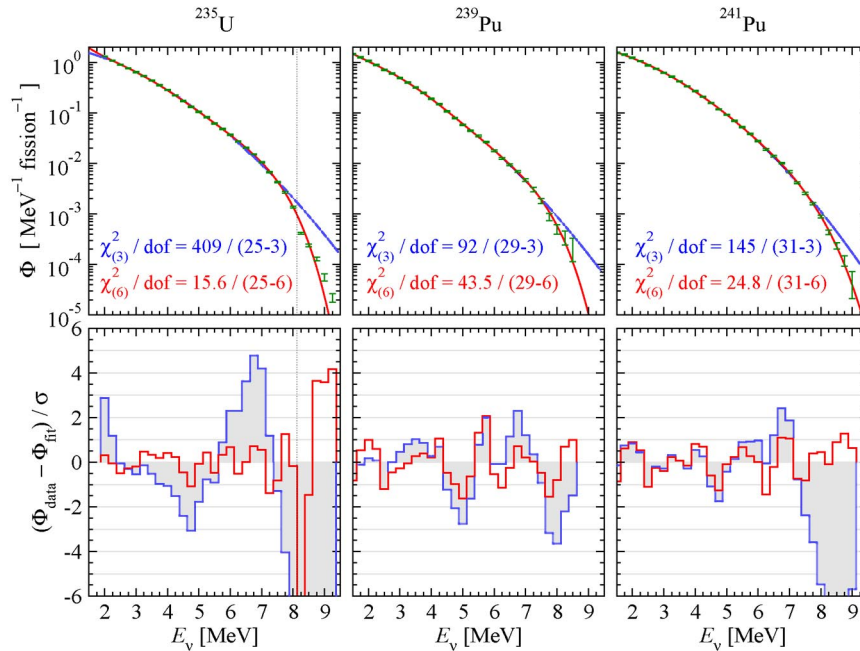


FIG. 1 (color online). Illustration of the fit to the data on the antineutrino spectra from ^{235}U [16], ^{239}Pu [17], and ^{241}Pu [17]. The thick/red curves correspond to a six parameter fit (polynomial of order 5), whereas the thin/blue curves correspond to a three parameter fit (polynomial of order 2). Also shown are the data with their 1σ error bars and the χ^2 per degree of freedom (number of data points minus fitted parameters). In the lower panels we show the residuals of the fits. Note that because of correlations the shown residuals do not add up to the given χ^2 -values. The data points to the right of the dotted line in the ^{235}U -panels are excluded from the fit.

TABLE III. Coefficients $a_{k\ell}$ of the polynomial of order 5 for the antineutrino flux from elements $\ell = {}^{235}\text{U}$, ${}^{239}\text{Pu}$, and ${}^{241}\text{Pu}$. In the column $\delta a_{k\ell}$ the 1σ errors on $a_{k\ell}$ are given. Furthermore the correlation matrix of the errors is shown.

$\ell = {}^{235}\text{U}$								
k	$a_{k\ell}$	$\delta a_{k\ell}$	1	2	3	4	5	6
1	3.519×10^0	7.26×10^{-1}	1.000	-0.996	0.987	-0.973	0.956	-0.938
2	-3.517×10^0	8.81×10^{-1}	-0.996	1.000	-0.997	0.989	-0.976	0.962
3	1.595×10^0	4.06×10^{-1}	0.987	-0.997	1.000	-0.997	0.990	-0.980
4	-4.171×10^{-1}	8.90×10^{-2}	-0.973	0.989	-0.997	1.000	-0.998	0.992
5	5.004×10^{-2}	9.34×10^{-3}	0.956	-0.976	0.990	-0.998	1.000	-0.998
6	-2.303×10^{-3}	3.77×10^{-4}	-0.938	0.962	-0.980	0.992	-0.998	1.000
$\ell = {}^{239}\text{Pu}$								
k	$a_{k\ell}$	$\delta a_{k\ell}$	1	2	3	4	5	6
1	2.560×10^0	4.01×10^{-1}	1.000	-0.993	0.977	-0.954	0.928	-0.899
2	-2.654×10^0	5.58×10^{-1}	-0.993	1.000	-0.995	0.982	-0.962	0.938
3	1.256×10^0	2.91×10^{-1}	0.977	-0.995	1.000	-0.996	0.984	-0.967
4	-3.617×10^{-1}	7.17×10^{-2}	-0.954	0.982	-0.996	1.000	-0.996	0.986
5	4.547×10^{-2}	8.37×10^{-3}	0.928	-0.962	0.984	-0.996	1.000	-0.997
6	-2.143×10^{-3}	3.73×10^{-4}	-0.899	0.938	-0.967	0.986	-0.997	1.000
$\ell = {}^{241}\text{Pu}$								
k	$a_{k\ell}$	$\delta a_{k\ell}$	1	2	3	4	5	6
1	1.487×10^0	3.23×10^{-1}	1.000	-0.991	0.974	-0.950	0.923	-0.893
2	-1.038×10^0	4.31×10^{-1}	-0.991	1.000	-0.994	0.980	-0.960	0.936
3	4.130×10^{-1}	2.15×10^{-1}	0.974	-0.994	1.000	-0.995	0.984	-0.966
4	-1.423×10^{-1}	5.02×10^{-2}	-0.950	0.980	-0.995	1.000	-0.996	0.986
5	1.866×10^{-2}	5.54×10^{-3}	0.923	-0.960	0.984	-0.996	1.000	-0.997
6	-9.229×10^{-4}	2.33×10^{-4}	-0.893	0.936	-0.966	0.986	-0.997	1.000

very well by the polynomial,³ although by accident the six parameter fit gives a reasonable approximation also in this energy range. Also for ${}^{241}\text{Pu}$ the high energy range $E_\nu \gtrsim 7$ MeV is important. In this case it is possible to obtain a good fit from the polynomial of order 5 even including the high energy part.

III. QUANTIFYING THE ANTI-NEUTRINO FLUX-UNCERTAINTIES

In this section we discuss in detail the uncertainties on the reactor antineutrino fluxes. In Table III, we show the errors $\delta a_{k\ell}$ on the coefficients of the polynomial as well as their correlation matrix $\rho_{kk'}^\ell$, as obtained from the fit to the measured beta spectra. Hence, the covariance matrix V^ℓ for the coefficients can be obtained by

$$V_{kk'}^\ell = \delta a_{k\ell} \delta a_{k'\ell} \rho_{kk'}^\ell. \quad (6)$$

From the table one observes that for a given element the coefficients are strongly correlated or anticorrelated, since for most elements of the correlation matrix we obtain $|\rho_{kk'}^\ell| \approx 1$. Therefore, we perform a rotation in the space of the $a_{k\ell}$, such that the covariance matrix

becomes diagonal. Let us for each isotope introduce new coefficients $c_{k\ell}$ by

$$a_{k\ell} = \sum_{k'} \mathcal{O}_{k'k}^\ell c_{k'\ell}, \quad (7)$$

where the orthogonal matrix \mathcal{O}^ℓ is defined by

$$\mathcal{O}^\ell V^\ell (\mathcal{O}^\ell)^T = \text{diag}[(\delta c_{k\ell})^2]. \quad (8)$$

Hence, the $\delta c_{k\ell}$ are the (uncorrelated) errors on the coefficients $c_{k\ell}$. Using Eqs. (4) and (7) the antineutrino flux for the isotope ℓ can be written as

$$\phi_\ell(E_\nu) = \exp \left[\sum_{k=1}^{K_\ell} c_{k\ell} p_k^\ell(E_\nu) \right], \quad (9)$$

where $p_k^\ell(E_\nu)$ is a polynomial of E_ν given by

$$p_k^\ell(E_\nu) = \sum_{k'=1}^{K_\ell} \mathcal{O}_{kk'}^\ell E_\nu^{k'-1}. \quad (10)$$

These polynomials describe the uncorrelated contributions to the error on the antineutrino flux. For example, let us consider some observable X , involving the antineutrino flux in the following way: $X = \int dE_\nu h(E_\nu) \phi_\ell(E_\nu)$, where $h(E_\nu)$ is some function of the neutrino energy. Then the error contribution from the coefficient $c_{k\ell}$ is given by

³In Ref. [14] a term of order E_ν^{10} is introduced to model this sharp falloff.

$$\delta X = \delta c_{k\ell} \frac{\partial X}{\partial c_{k\ell}} = \int dE_\nu h(E_\nu) \phi_\ell(E_\nu) \delta c_{k\ell} p_k^\ell(E_\nu). \quad (11)$$

Hence, the product $\delta c_{k\ell} p_k^\ell(E_\nu)$ is a measure for the importance of the error $\delta c_{k\ell}$ for any observable. In the upper panel of Fig. 2 we show the polynomials Eq. (10) weighted by the corresponding error for ^{235}U . For ^{239}Pu and ^{241}Pu we obtain very similar results. One observes that in the relevant range of the antineutrino energy the flux-uncertainties are at the level of 2%. The weighted polynomials $\delta c_{k\ell} p_k^\ell(E_\nu)$ for the isotopes ^{235}U , ^{239}Pu , ^{241}Pu are available in computer readable format at the web-page Ref. [23]. Once these functions are known, the flux-uncertainties on any observable can be included similar to Eq. (11).

As first simple application let us mention how one can calculate the number of antineutrinos per fission N_ℓ^ν above the threshold and its uncertainty, as given in Table I. Given the best-fit parameters and their covariance matrix for ^{235}U , ^{239}Pu , ^{241}Pu we readily obtain

$$N_\ell^\nu = \int_{1.8 \text{ MeV}}^{\infty} \phi_\ell(E_\nu) dE_\nu, \quad (12)$$

$$(\delta N_\ell^\nu)^2 = \sum_{kk'} \frac{\partial N_\ell^\nu}{\partial a_{k\ell}} \frac{\partial N_\ell^\nu}{\partial a_{k'\ell}} V_{kk'}^\ell = \sum_k \left(\frac{\partial N_\ell^\nu}{\partial c_{k\ell}} \delta c_{k\ell} \right)^2.$$

In addition to the three isotopes ^{235}U , ^{239}Pu , and ^{241}Pu , ^{238}U also gives a contribution of a few percent to the

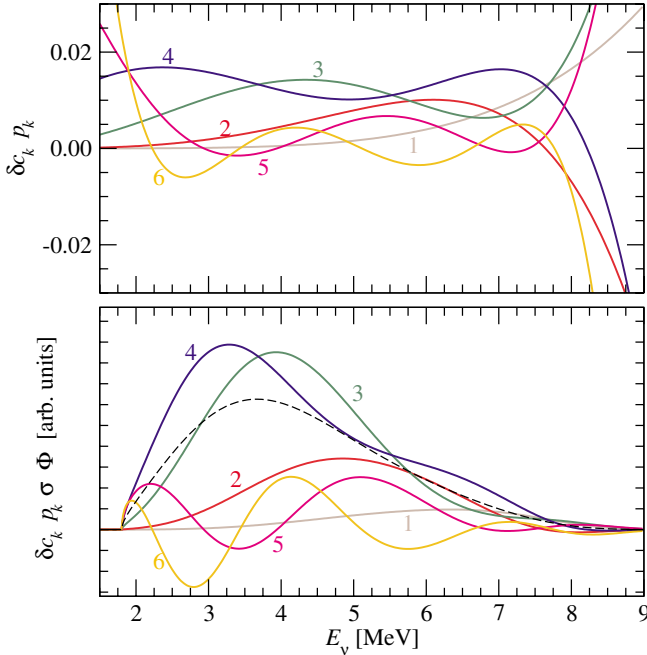


FIG. 2 (color online). Uncorrelated antineutrino flux-uncertainties for ^{235}U . The upper panel shows the polynomials $p_k^\ell(E_\nu)$ given in Eq. (10) multiplied by the corresponding error $\delta c_{k\ell}$. The lower panel shows the functions $\delta c_{k\ell} p_k^\ell(E_\nu) \sigma(E_\nu) \phi_\ell(E_\nu)$, where $\sigma(E_\nu)$ is the detection cross section. The dashed curve corresponds to $\sigma(E_\nu) \phi_\ell(E_\nu)/100$.

reactor antineutrino flux. For this isotope no measurements exist and one has to rely on theoretical calculations [20,21]. In the following we will always adopt for ^{238}U the parameterization with the second order polynomial given in Ref. [22], which we reproduce in the last row of Table II. In particular, that parameterization has been used to calculate also the value of N_ℓ^ν for ^{238}U given in Table I; the error of 2% is an educated guess motivated by the errors obtained for the other isotopes. Since no covariance matrix of the flux coefficients for ^{238}U is available we will always assume in the following that they are known exactly. Since the contribution of ^{238}U to the total flux is rather small, this assumption has very little impact on the conclusions drawn in this work.

IV. THE IMPACT OF ANTI-NEUTRINO FLUX-UNCERTAINTIES IN KAMLAND

The KamLAND [6,7] reactor-neutrino experiment is located in the Kamioka mine in Japan and observes the electron antineutrinos emitted by ~ 16 nuclear power plants at distances of ~ 200 km. The results of KamLAND have provided convincing evidence for $\bar{\nu}_e$ disappearance and are in agreement with the so-called LMA-MSW solution of the solar neutrino problem (see, e.g., Ref. [24]). The neutrino oscillation analysis of current KamLAND data is dominated by statistical errors⁴ and it is a good approximation to gather various sources of systematical errors into an uncertainty on the overall number of events. However, in the future, if more data are accumulated statistical errors will decrease and in principle one has to treat systematical errors more carefully. In this section we investigate the impact of uncertainties on the antineutrino flux for the determination of oscillation parameters in KamLAND. To this end we naively extrapolate the size of the data sample published in Ref. [6] to a total of five years data taking time by multiplying the event numbers by the factor $5 \times 356/145.1$, where 145.1 days is the exposure time of the reference sample. For further details on the KamLAND analysis see Refs. [24,25].

In the case of KamLAND one has to generalize the expression for the number of events per positron energy bin from Eq. (3) to account for the fact that several reactors (labeled by the index r) at different distances L_r contribute to the signal, and that neutrino oscillations occur:

$$N_i = \mathcal{N} \sum_r \frac{P_r}{L_r^2} \sum_\ell \frac{f_{r\ell}}{E_\ell} \times \int dE_\nu \sigma(E_\nu) \phi_\ell(E_\nu) R_i(E_\nu) P_{ee}(L_r/E_\nu). \quad (13)$$

⁴The robustness of the KamLAND results with respect to statistical fluctuations has been extensively discussed in Ref. [25].

Here \mathcal{N} is a normalization constant, P_r and $f_{r\ell}$ are the power output and the element composition of the reactor r , respectively, and P_{ee} is the oscillation probability depending on the neutrino mass-squared difference Δm^2 and the mixing angle θ . In our analysis we consider the following contributions to the covariance matrix V^{KL} of the event numbers N_i :

$$V_{ij}^{\text{KL}} = N_i \delta_{ij} + N_i N_j \sigma_{\text{det}}^2 + V_{ij}^{\text{flux}}, \quad (14)$$

where the first term of the right hand side is the statistical error and the second term accounts for the overall normalization error σ_{det} . The uncertainties on the antineutrino flux are included in V^{flux} , which we take as

$$V_{ij}^{\text{flux}} = \sum_r \frac{\partial N_i}{\partial P_r} \frac{\partial N_j}{\partial P_r} (\delta P_r)^2 + \sum_{r\ell} \frac{\partial N_i}{\partial f_{r\ell}} \frac{\partial N_j}{\partial f_{r\ell}} (\delta f_{r\ell})^2 + \sum_{k\ell} \frac{\partial N_i}{\partial c_{k\ell}} \frac{\partial N_j}{\partial c_{k\ell}} (\delta c_{k\ell})^2. \quad (15)$$

Here δP_r and $\delta f_{r\ell}$ are the errors on the power output and isotope composition of each reactor, and we assume typical values of $(\delta P_r)/P_r = 0.02$ and $(\delta f_{r\ell})/f_{r\ell} = 0.01$. These errors are taken uncorrelated between the reactors. The last term in Eq. (15) takes into account the uncertainty on the coefficients of the parameterization for the antineutrino fluxes as discussed in Sec. III.

In Fig. 3 we show the 3σ allowed regions for the oscillation parameters after five years of KamLAND data for various assumptions about the systematic errors. We observe from this figure that even after five years the KamLAND analysis is dominated by the statistical and the overall normalization errors. The shaded region corresponds to statistical errors only, for the thin solid curve only the normalization error of $\sigma_{\text{det}} = 6.42\%$ [6] is included. In Table two of Ref. [6] various contributions to σ_{det} are listed. If the uncertainties related to the flux are subtracted σ_{det} is reduced to 5.46% (see blue/dashed curve in Fig. 3). For the red/solid and green/dash-dotted curves, the flux-uncertainties according to Eq. (15) are included as well. In both cases we find a very small effect on the oscillation parameters.

To summarize, we find that even for five years of KamLAND data the determination of the oscillation parameters is dominated by statistical and overall normalization errors. The effect of flux-uncertainties is rather small, and, in particular, it is not necessary to fully take into account flux shape errors. The inclusion of only the normalization errors for the total flux from each element (see Table I) leads to nearly identical results as accounting for the full covariances of the coefficients $a_{k\ell}$. However, the proper treatment of the flux-uncertainties reduces the overall normalization error. This will become more relevant if in future KamLAND analyses normalization errors like the uncertainty on the fiducial volume will be reduced. This will be relevant mainly for the

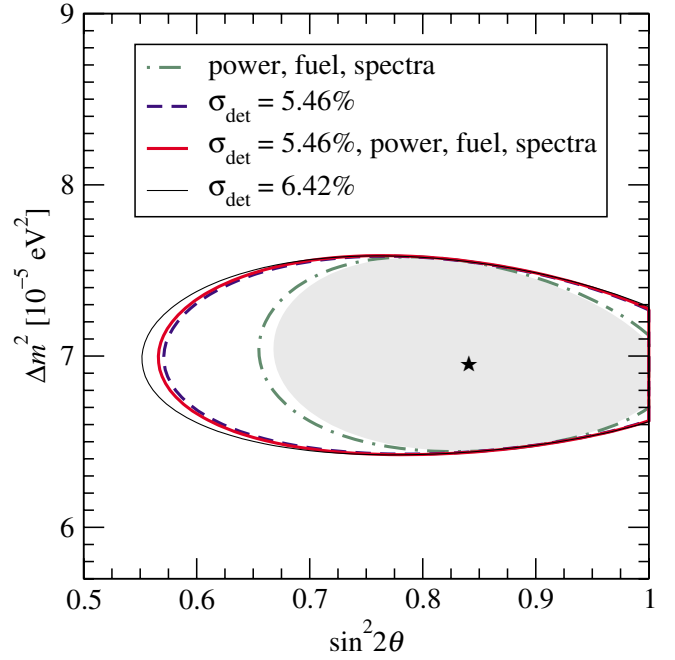


FIG. 3 (color online). 3σ allowed regions for $\sin^2 2\theta$ and Δm^2 after five years of KamLAND data. The shaded region corresponds to statistical errors only, the regions delimited by the curves correspond to various assumptions about systematical errors. σ_{det} is a fully correlated error on the overall normalization. For the curves labeled “power, fuel, spectra” we include a 2% error on the power output of each reactor, 1% error on the fuel composition of each reactor, and the uncertainty on the antineutrino spectrum as described in the text.

measurement of the mixing angle, the determination of Δm^2 is hardly affected by any of the systematical errors.

Finally, we note already that for the current KamLAND data sample [7] small differences in the allowed regions are visible due to the use of our neutrino fluxes, compared to the parameterization of Ref. [22]. For completeness, we mention that additional effects like the time evolution of the individual reactor powers or isotope compositions due to burn-up [26] may become relevant for future KamLAND analyses. The investigation of such effects is beyond the scope of the present work.

V. APPLICATION TO FUTURE REACTOR EXPERIMENTS TO MEASURE θ_{13}

Let us now discuss the relevance of the flux-uncertainties for reactor experiments planned to measure the small leptonic mixing angle θ_{13} . It has been realized that the bound on this angle from previous experiments [4,5] can be significantly improved if in addition to a far detector at a distance of order 2 km from the reactor a near detector at a few hundred meters is used. Because of the large number of events, the near detector provides accurate information on the reactor-neutrino flux.

Identical near and far detectors with normalization errors σ_{det} below 1% will provide an accuracy on $\sin^2 2\theta_{13}$ of order 0.01 (see, e.g., Refs. [9,27–30]).

In Fig. 4 we show the difference between the positron spectra predicted for no oscillations from the three and six parameter description of the neutrino spectra. The comparison with the statistical accuracy for a total number of events of 40 000, which is typical for the far detector of these experiments [9], shows that for such experiments a precise model for the flux is needed. The small differences between the two parameterizations are clearly distinguishable by the statistical precision in the far detector; For 60 bins in positron energy we obtain $\chi^2/\text{dof} = 139/60$, where $\chi^2 = \sum_i [N_i^{(6P)} - N_i^{(3P)}]^2 / N_i^{(6P)}$. Note that in the near detector χ^2 is much worse, because of the larger number of events.

In the following we adopt the six parameter model for the neutrino fluxes and investigate the impact of the errors of the coefficients on the sensitivity to the mixing angle. For simplicity we consider here only two-flavour neutrino oscillations characterized by the mixing angle θ and the neutrino mass-squared difference Δm^2 . The number of events in a given positron energy bin i in the detector A ($A = N, F$) can be calculated by

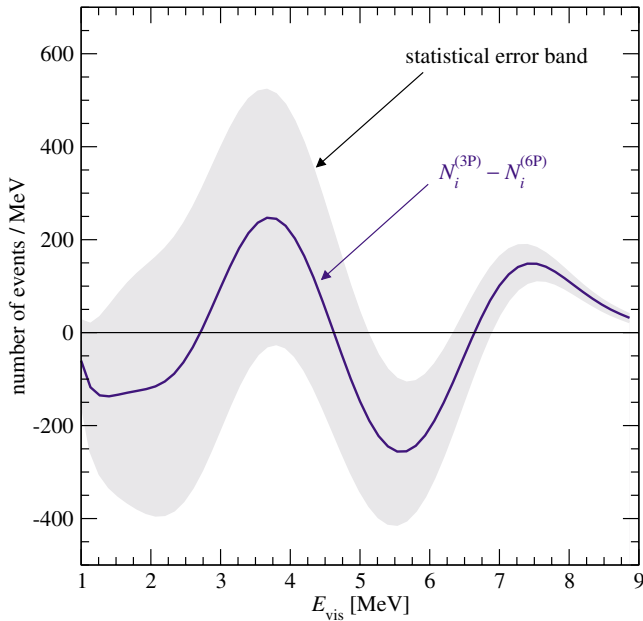


FIG. 4 (color online). Difference between the positron spectra for no oscillations $N_i^{(3P)}$ and $N_i^{(6P)}$, obtained by using the three parameter fit (Table II) and six parameter fit (Table III) to the antineutrino spectra, respectively. We assume a total number of events of 40 000 and a typical isotope composition of ^{235}U : ^{239}Pu : ^{238}U : ^{241}Pu = 0.57: 0.30: 0.08: 0.06. The shaded area corresponds to the 1σ statistical error band, i.e., $\pm\sqrt{N_i^{(6P)}}$. For 60 bins in positron energy and statistical errors only we find $\chi^2/\text{dof} = 139/60$.

$$N_i^A = P \frac{\mathcal{N}_A}{L_A^2} \sum_{\ell} \frac{f_{\ell}}{E_{\ell}} \times \int dE_{\nu} \sigma(E_{\nu}) \phi_{\ell}(E_{\nu}) R_i(E_{\nu}) P_{ee}(L_A/E_{\nu}). \quad (16)$$

Similar to Ref. [27] we take into account the various systematical errors by writing

$$T_i^A = (1 + a + b_A) N_i^A + g_A M_i^A + \sum_{\ell} \zeta_{\ell} f_{\ell} \frac{\partial N_i^A}{\partial f_{\ell}} + \sum_{k\ell} \xi_{k\ell} \delta c_{k\ell} \frac{\partial N_i^A}{\partial c_{k\ell}}. \quad (17)$$

Here the parameters a and b_A describe the uncertainty on the reactor power and the detector normalizations, respectively. The term $g_A M_i^A$ accounts for the energy calibration (see Ref. [27] for details) and the last two terms in Eq. (17) describe the uncertainty on the isotope fractions and the coefficients $c_{k\ell}$, respectively. To test the oscillation parameters we consider the χ^2

$$\chi^2 = \sum_{i,A} \frac{(T_i^A - O_i^A)^2}{O_i^A} + \left(\frac{a}{\sigma_a}\right)^2 + \sum_A \left[\left(\frac{b_A}{\sigma_{\text{det}}}\right)^2 + \left(\frac{g_A}{\sigma_{\text{cal}}}\right)^2 \right] + \sum_{\ell} \left(\frac{\zeta_{\ell}}{\sigma_f}\right)^2 + \sum_{k\ell} \xi_{k\ell}^2, \quad (18)$$

where the T_i^A depend on θ and Δm^2 , whereas $O_i^A = N_i^A(\theta = \Delta m^2 = 0)$. For each value of θ and Δm^2 Eq. (18) has to be minimized with respect to the ‘‘pulls’’ $a, b_A, g_A, \zeta_{\ell}, \xi_{k\ell}$.

In Fig. 5 we show the results of this analysis for a wide range of Δm^2 . The values of Δm^2 relevant for the θ_{13} measurement are constrained by atmospheric neutrino data to the interval $1.4 \times 10^{-3} \text{ eV}^2 \leq \Delta m^2 \leq 3.6 \times 10^{-3} \text{ eV}^2$ at 3σ (shaded region in Fig. 5). The regions of Δm^2 up to 1 eV^2 could be relevant for oscillations into hypothetical sterile neutrinos [31,32]. The solid curves in Fig. 5 are calculated for perfectly known antineutrino flux, i.e., by fixing the coefficients $\xi_{k\ell}$ in Eqs. (17) and (18) to zero. For the dashed curves we use the errors obtained in the fit to the beta spectra as discussed in Sec. III. For the dotted curves the antineutrino flux coefficients are treated as free parameters in the fit, i.e., we drop the last term in Eq. (18) when minimizing with respect to $\xi_{k\ell}$. In Fig. 5 we consider two experimental configurations. One corresponds to an experiment with 6×10^4 events in the far detector for no oscillations and near and far detector baselines of $L_{\text{ND}} = 0.15 \text{ km}$ and $L_{\text{FD}} = 1.05 \text{ km}$. This set-up is similar to the Double-Chooz proposal [30]. For the second configuration we have assumed a somewhat larger near detector baseline of $L_{\text{ND}} = 0.7 \text{ km}$, a far detector baseline optimized for $\Delta m^2 \sim 2 \times 10^{-3} \text{ eV}^2$ of $L_{\text{ND}} = 1.7 \text{ km}$, and a rather high luminosity of 6×10^5 events.

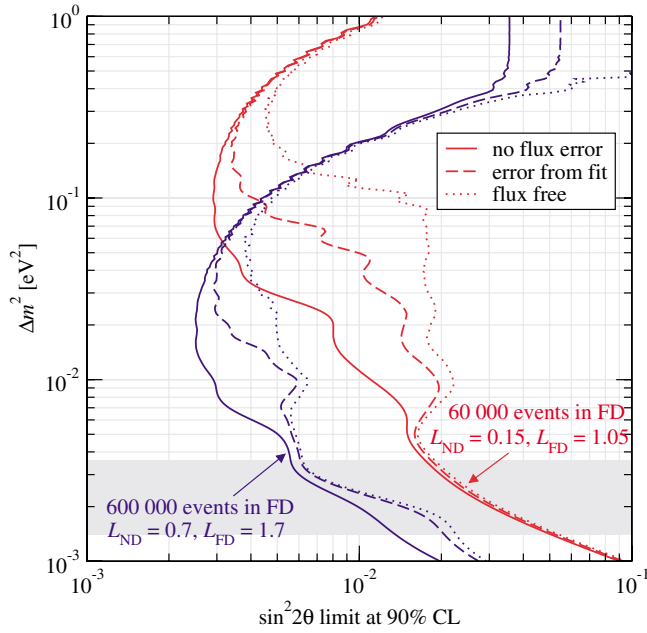


FIG. 5 (color online). The 90% CL limit on $\sin^2 2\theta$ from reactor-neutrino experiments with near and far detectors as a function of Δm^2 . The bound is shown for two experimental configurations as indicated in the figure. The solid curves correspond to no errors on the reactor-neutrino flux, for the dashed curves the covariance matrix from the fit to the beta spectra is used, and for the dotted curves the coefficients for the antineutrino flux are treated as free parameters in the fit. In all cases we have assumed $\sigma_a = 1\%$ for the uncertainty of the reactor power, $\sigma_{\text{det}} = 0.6\%$ for the detector normalization, $\sigma_{\text{cal}} = 0.5\%$ for the energy calibration, and $\sigma_f = 1\%$ for the error on the isotope fractions. The shaded region indicates the range of Δm^2 allowed at 3σ from atmospheric neutrino data.

Let us first discuss the region of Δm^2 relevant for the θ_{13} measurement. We observe from the figure that in the case of $L_{\text{ND}} = 0.15$ km the limit does hardly depend on the assumptions concerning the flux uncertainty. Even the flux free limit is not much worse than the limit for no error on the flux, since at these short distances the near detector provides a very accurate determination of the antineutrino flux. In contrast, the flux uncertainty has some impact on the θ_{13} measurement if the near detector baseline is somewhat larger. In that case oscillations start to build up already between reactor and near detector and the uncertainties on the initial flux become relevant (see also Fig. 12 in Ref. [27]). In the region $\Delta m^2 \geq 5 \times 10^{-3}$ eV² the main information relevant for the limit is provided by the near detector. Hence the flux-uncertainties become even more relevant for both configurations in that region. We note that around $\Delta m^2 \sim 2(7) \times 10^{-1}$ eV² for the big (small) experiment the limit again becomes independent of the flux uncertainty. In that region rather fast oscillations occur at the near detector

which still can be resolved by the detector, but cannot be mimicked by adjusting the coefficients of the flux parameterization. Obviously, no limit can be obtained for the flux free analysis in the averaging regime of very high Δm^2 .

VI. POTENTIAL OF AN ANTI-NEUTRINO DETECTOR CLOSE TO A REACTOR

In this section we investigate the potential of an anti-neutrino detector very close to a reactor, where “very close” is defined by the requirement that neutrino oscillations do not occur. This could be, for example, a near detector of the experiments considered in the previous section, if it is situated close enough to the reactor. In Section VIA we investigate to what extent the uncertainty on the antineutrino flux can be reduced by such a measurement, whereas in Section VIB we consider the possibility to determine the isotope composition of the reactor core.

To this aim we write the theoretical prediction for the number of events in bin i given in Eq. (17) as

$$T_i = O_i + \sum_{\alpha} p_{\alpha} \Phi_{\alpha}^i, \quad (19)$$

where we drop the detector index A and we use the fact that $N_i = O_i$ for no oscillations. The index α runs over all the pulls: $p_{\alpha} = (a, b, g, \zeta_{\ell}, \xi_{k\ell})$ and the coefficients Φ_{α}^i can be read off from Eq. (17). With this notation Eq. (18) becomes

$$\chi^2 = \sum_i \frac{(\sum_{\alpha} p_{\alpha} \Phi_{\alpha}^i)^2}{O_i} + \sum_{\alpha} \left(\frac{p_{\alpha}}{\delta p_{\alpha}} \right)^2, \quad (20)$$

where δp_{α} is the error on the pull p_{α} , which can be read off from Eq. (18). Departing from Eq. (20) it is straight forward to compute the improvement of the knowledge on a given parameter p_{α} due to the data O_i : Because of the quadratic structure of Eq. (20) the new covariance matrix S^{new} of the p_{α} can be obtained by inverting

$$(S^{\text{new}})_{\alpha\beta}^{-1} = \frac{1}{2} \frac{\partial^2 \chi^2}{\partial p_{\alpha} \partial p_{\beta}} = \delta_{\alpha\beta} \frac{1}{(\delta p_{\alpha})^2} + \sum_i \frac{\Phi_{\alpha}^i \Phi_{\beta}^i}{O_i}. \quad (21)$$

Note that in general the p_{α} will be correlated after the measurement, i.e., S^{new} will acquire nondiagonal entries from the second term in Eq. (21). The final one sigma error on a parameter p_{α} is given by $\sqrt{S_{\alpha\alpha}^{\text{new}}}$.

A. Improving Our Knowledge on the Anti-Neutrino Flux

From Fig. 5 one can see that the limit on the mixing angle is nearly the same for an analysis with completely free antineutrino flux coefficients (dotted curves) and for the current errors on them (dashed curves), in the region $\Delta m^2 \lesssim 10^{-2}$ eV², where oscillations can be neglected in

the near detector. This indicates that the near detector provides a rather precise determination of the flux on its own.

This fact is quantified in Fig. 6, where we show the improvement of the flux errors for ^{235}U from the near detector data with respect to the present errors obtained from the fit to the beta spectra measurements. We observe from the figure that for a number of events $\geq 10^4$ the errors on the flux coefficients from the antineutrino measurement become comparable to the current errors. To reduce the errors by a factor two roughly 10^7 events are needed. To avoid correlations with the flux coefficients from other isotopes, we assume that the core contains practically only ^{235}U . However, for large number of events the errors on the coefficients $c_{k\ell}$ become strongly correlated. Especially the coefficients corresponding to the lines labeled “2”, “3” and “4” in Fig. 6 are nearly fully correlated. This implies that a certain combination of these coefficients is severely constrained, and one should perform a diagonalization of the covariance matrix (similar as described in Section III) to obtain again uncorrelated flux-uncertainties in analogy to Fig. 2. Note that the modes labeled “5” and “6” corresponding to relatively “fast oscillations” (compare Fig. 2) can be determined rather well by the antineutrino measurement. We find only modest correlations of these coefficients.

In general also sizable fractions of ^{239}Pu , ^{238}Pu , and ^{238}U will be present in the reactor. In this case all coefficients will become correlated. It might be possible to

disentangle the contributions of the various isotopes taking into account precise information on the time evolution of the reactor composition. The improvement for a given isotope depends strongly on the relative amount of this isotope in the core.

B. Determination of the Isotope Composition of a Reactor

In this section we investigate the possibility to determine the isotope composition of a reactor core by a nearby antineutrino detector. This could lead to applications of neutrino spectroscopy for reactor monitoring, either for improving the reliability of operation of power reactors or as a method to accomplish certain safeguard and nonproliferation objectives. In both cases the price tag of a moderately sized detector is small compared to the overall cost or benefit. Therefore the applicability of neutrino spectroscopy seems to depend only on its performance compared to existing technologies. For example the accuracy in the determination of the thermal power of civil power reactors as used for the production of electricity typically is in the range 0.6% – 1.5% [5]. The isotopic composition usually is not measured *in situ* but deduced from the time development of the reactor thermal power and the initial isotopic composition by using detailed reactor core simulation tools and is typically accurate at the percent level [11].

On the other hand, one requires for safeguard purposes to achieve a sensitivity which allows to quickly detect the diversion of weapons grade material at the level of one critical mass [10], e.g., for Plutonium this is approximately 10 kg. The average power reactor contains three tons of fissionable material of which roughly 40% have been converted to Plutonium by the end of the fuel lifetime, thus 10 kg Plutonium correspond to $\sim 0.8\%$ of the total content of Plutonium, which is beyond the accuracy levels for *in situ* monitoring today. The determination of the isotopic composition by the traditional methods furthermore relies on the assumption that the operator of the reactor collaborates. In the following we will show that neutrino spectroscopy has the potential to reach a sensitivity comparable to existing technologies and it does *not* require detailed information on the power history or the initial fuel composition, which is an important advantage especially in safeguards applications. In contrast to the existing literature on this topic [10–12] we use the full spectral information and therefore do not require an independent determination of the reactor power. In general, any safeguard regime based only on the total rate suffers from two problems: The first one is related to the availability of reliable information on the thermal power, whereas the second one is related to the fact that for most reactor types the diversion of core inventory is only possible during refueling, i.e., when the reactor is

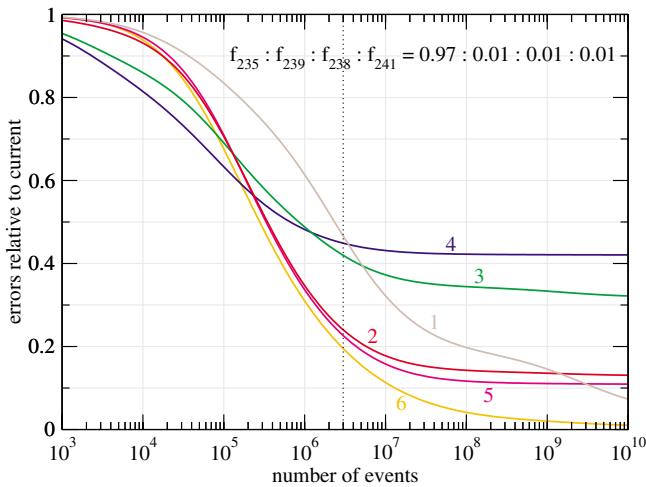


FIG. 6 (color online). Improvement for the antineutrino flux errors for ^{235}U as a function of the total number of events in a detector close to a reactor. We show $\sqrt{S_{\alpha\alpha}^{\text{new}}}$, where S^{new} is defined in Eq. (21) and α runs over the six pulls associated with the flux-uncertainties shown in Fig. 2. We assume that the core contains 97% ^{235}U , and we take $\sigma_a = 1\%$, $\sigma_{\text{det}} = 0.6\%$, $\sigma_{\text{cal}} = 0.5\%$, and $\sigma_f = 1\%$. The dotted line corresponds roughly to the number of events expected in the near detector of the Double-Chooz experiment [30].

switched off and there is no neutrino flux. Thus in order to detect any diversion in this period an absolute measurement of the neutrino flux as well as of the thermal power is required. Moreover the composition of the new fuel has to be known exactly in order to predict the spectrum which is expected in case of no diversion.

In the following we perform a fit where the isotope fractions f_ℓ are treated as free parameters, subject to the condition $\sum f_\ell = 1$. We impose no external information on the reactor power, i.e., no knowledge at all about the reactor is assumed. This means that we set $1/(\delta p_\alpha)^2 = 0$ in Eq. (21) for α corresponding to σ_a and σ_f . The determination of the isotope fractions and the power is solely based on the differences between the antineutrino spectra emitted by the four isotopes. In Fig. 7 we show the 1σ accuracy obtained on the isotope fractions and the reactor power as a function of the antineutrino events. To give an example, for a detector with 1 ton fiducial mass at a distance of ten meters from a reactor with three GW thermal power roughly 10^6 events are expected within three months of measurement time.

First, one can see from Fig. 7 that for $\geq 10^5$ events a rather precise determination of the reactor power at the $\approx 3\%$ level is possible, given the current uncertainty on the antineutrino fluxes. For perfectly known fluxes the power accuracy is limited by the systematical uncertainty of the detector normalization. Second, for $\geq 10^6$ events also the isotope fractions of ^{235}U , ^{239}Pu , and ^{241}Pu can be determined at the percent level if no errors on the antineutrino fluxes are taken into account.⁵ The accuracy on the sum of the ^{239}Pu and ^{241}Pu fractions is clearly better than the one on the individual fractions. This is a consequence of the strong anticorrelation between the two Pu isotopes, which we illustrate in Fig. 8, where χ^2 contours in the ^{239}Pu - ^{241}Pu plane are shown for 10^6 events. Note that for safeguard applications actually the sum of both Plutonium isotopes is the interesting quantity.

From Fig. 7 one can see that to determine the isotope composition a precise knowledge of the emitted fluxes is necessary. With present errors the 1σ accuracy is limited to $\approx 10\%$. To reach a determination at the percent level the errors on the coefficients of the flux parameterization have to be reduced by a factor of 3 to 10. A factor 3 would be approximately achieved by the near detector of an experiment like Double-Chooz [30].

Let us note that in this analysis we do not take into account additional information such as the time evolution and reactor burn-up, or information from various traditional safeguard methods. The main conclusion from the above results is that antineutrino spectroscopy may play an important role for reactor monitoring, especially since

⁵We consider the fractions of ^{235}U , ^{239}Pu , and ^{241}Pu as independent parameters, and determine the ^{238}U fraction by the constraint $\sum f_\ell = 1$.

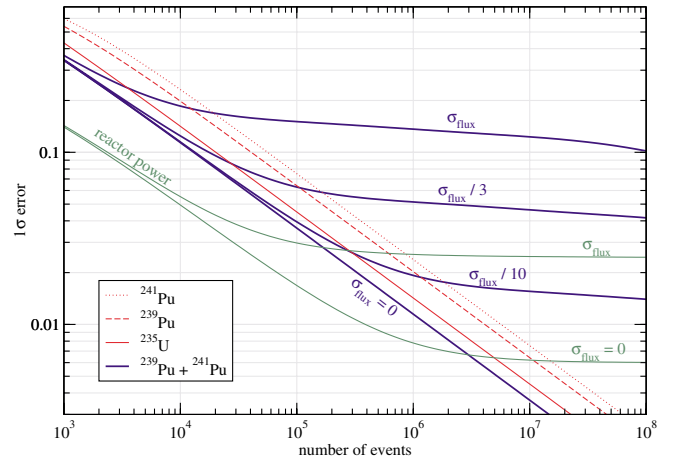


FIG. 7 (color online). The 1σ error on the fraction of ^{235}U , ^{239}Pu , and ^{241}Pu as a function of the number of antineutrino events. The thick curves correspond to the error on the sum of ^{239}Pu and ^{241}Pu . The straight lines are calculated for perfectly known antineutrino fluxes. For the sum of ^{239}Pu and ^{241}Pu we show also the result assuming the present antineutrino flux-uncertainties (“ σ_{flux} ”), and uncertainties reduced by factors three (“ $\sigma_{\text{flux}}/3$ ”) and ten (“ $\sigma_{\text{flux}}/10$ ”). Also shown is the relative 1σ error on the reactor power for $\sigma_{\text{flux}} = 0$ and present flux errors. We assume an isotope composition ^{235}U : ^{239}Pu : ^{238}U : ^{241}Pu = 0.4: 0.4: 0.1 and a detector normalization uncertainty $\sigma_{\text{det}} = 0.6\%$.

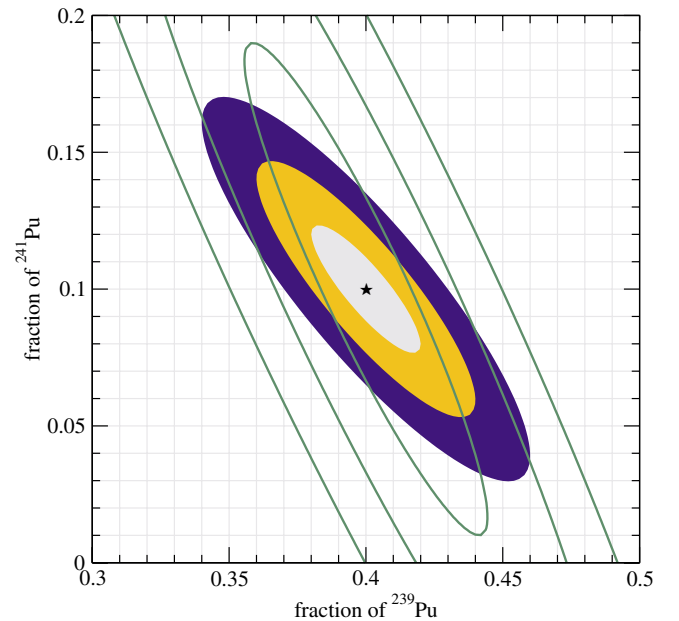


FIG. 8 (color online). Contours of $\Delta\chi^2 = 1, 4, 9$ in the plane of the ^{239}Pu and ^{241}Pu isotope fractions for 10^6 antineutrino events. The colored regions correspond to perfectly known antineutrino flux shapes, whereas for the curves we assume uncertainties on the flux coefficients 3 times smaller than the present errors. We adopt the same isotope composition and σ_{det} as in Fig. 7. Reactor power and ^{235}U fraction are treated as free parameters.

one expects significant synergies due to the combination with alternative technologies.

VII. SUMMARY AND CONCLUSIONS

In this work we have presented an accurate parameterization of the antineutrino flux produced by the isotopes ^{235}U , ^{239}Pu , and ^{241}Pu in nuclear reactors. We use a polynomial of order 5 and determine the coefficients by performing a fit to spectra inferred from experimentally measured beta spectra. Furthermore, the correlated errors on these coefficients are determined from the fit.

Subsequently we investigate the impact of the flux-uncertainties for the KamLAND experiment and future reactor experiments to measure the mixing angle θ_{13} . We show that flux shape uncertainties can be safely neglected in the KamLAND experiment, however the proper treatment of the errors associated with the antineutrino flux reduces somewhat the overall systematic error in KamLAND, which has some impact on the determination of the mixing angle. Future high precision reactor-neutrino experiments with a far detector at distances of order 2 km and a near detector at hundreds of meters are sensitive to the fine details of the reactor-neutrino spectra. We find that a parameterization based on a polynomial of order 2 is not accurate enough to describe the antineutrino spectrum at the required level of precision. If the near detector is located at distances ≥ 500 meters the flux-uncertainties are relevant for the θ_{13} measurements. Moreover, in searches for sterile neutrinos at values of

$\Delta m^2 \gtrsim 10^{-2} \text{ eV}^2$ the main information is provided by the near detector, and hence the inclusion of antineutrino flux-uncertainties is essential.

Finally, we have investigated the potential of a detector very close to a reactor to improve on the uncertainties of the antineutrino fluxes, and to determine the isotopic composition in nuclear reactors through an antineutrino measurement. We find that without any external knowledge on the reactor a three month exposure of a 1 ton detector allows the determination of the isotope fractions and the thermal reactor power at a few percent accuracy. This may open the possibility of an application for safeguard or nonproliferation objectives, which does not rely on information on the reactor thermal power or on the initial fuel composition, and hence neutrino spectroscopy can provide information complementary to traditional monitoring methods. To achieve this goal a reduction of the present errors on the antineutrino fluxes of about a factor of 3 is necessary, which naturally can be obtained from the data of the near detector of a Double-Chooz like experiment.

ACKNOWLEDGMENTS

We thank Michele Maltoni for discussions on the KamLAND analysis, and Hervé de Kerret for communication on the CHOOZ experiment. This work has been supported by the ‘‘Sonderforschungsbereich 375 für Astro-Teilchenphysik der Deutschen Forschungsgemeinschaft’’.

-
- [1] C. L. Cowan, F. Reines, F. B. Harrison, H.W. Kruse, and A. D. McGuire, *Science* **124**, 103 (1956).
 - [2] CALTECH-SIN-TUM, G. Zacek *et al.*, *Phys. Rev. D* **34**, 2621 (1986).
 - [3] Y. Declais *et al.*, *Nucl. Phys. B* **434**, 503 (1995).
 - [4] F. Boehm *et al.*, *Phys. Rev. D* **64**, 112001 (2001).
 - [5] M. Apollonio *et al.*, *Eur. Phys. J. C* **27**, 331 (2003).
 - [6] KamLAND, K. Eguchi *et al.*, *Phys. Rev. Lett.* **90**, 021802 (2003).
 - [7] KamLAND, T. Araki *et al.* (to be published).
 - [8] C. Bemporad, G. Gratta, and P. Vogel, *Rev. Mod. Phys.* **74**, 297 (2002).
 - [9] K. Anderson *et al.*, hep-ex/0402041.
 - [10] A. Bernstein, Y. Wang, G. Gratta, and T. West, *J. Appl. Phys.* **91**, 4672 (2002).
 - [11] M. M. Nieto, A. C. Hayes, C. M. Teeter, W. B. Wilson, and W. D. Stanbro, nucl-th/0309018.
 - [12] V. D. Rusov, T. N. Zelentsova, V. A. Tarasov, and D. A. Litvinov, hep-ph/0403207.
 - [13] P. Vogel and J. F. Beacom, *Phys. Rev. D* **60**, 053003 (1999).
 - [14] V. I. Kopeikin, L. A. Mikaelyan, and V. V. Sinev, *Phys. At. Nucl.* **60**, 172 (1997).
 - [15] V. Kopeikin, L. Mikaelyan, and V. Sinev, hep-ph/0308186.
 - [16] K. Schreckenbach, G. Colvin, W. Gelletly, and F. Von Feilitzsch, *Phys. Lett. B* **160**, 325 (1985).
 - [17] A. A. Hahn *et al.*, *Phys. Lett. B* **218**, 365 (1989).
 - [18] F. Von Feilitzsch, A. A. Hahn, and K. Schreckenbach, *Phys. Lett. B* **118**, 162 (1982).
 - [19] B. Achkar *et al.*, *Phys. Lett. B* **374**, 243 (1996).
 - [20] P. Vogel, G. K. Schenter, F. M. Mann, and R. E. Schenter, *Phys. Rev. C* **24**, 1543 (1981).
 - [21] H. V. Klapdor and J. Metzinger, *Phys. Lett. B* **112**, 22 (1982).
 - [22] P. Vogel and J. Engel, *Phys. Rev. D* **39**, 3378 (1989).
 - [23] Web-p.: <http://www.ph.tum.de/~schwetz/reactor-neutrino-data/>.
 - [24] M. Maltoni, T. Schwetz, and J. W. F. Valle, *Phys. Rev. D* **67**, 093003 (2003).
 - [25] T. Schwetz, *Phys. Lett. B* **577**, 120 (2003).

- [26] H. Murayama and A. Pierce, *Phys. Rev. D* **65**, 013012 (2002).
- [27] P. Huber, M. Lindner, T. Schwetz, and W. Winter, *Nucl. Phys. B* **665**, 487 (2003).
- [28] H. Minakata, H. Sugiyama, O. Yasuda, K. Inoue, and F. Suekane, *Phys. Rev. D* **68**, 033017 (2003).
- [29] V. Martemyanov, L. Mikaelyan, V. Sinev, V. Kopeikin, and Y. Kozlov, *Phys. At. Nucl.* **66**, 1934 (2003).
- [30] F. Ardellier *et al.* (2004), hep-ex/0405032.
- [31] L. Mikaelyan and V. Sinev, *Phys. At. Nucl.* **62**, 2008 (1999).
- [32] V. Kopeikin, L. Mikaelyan, and V. Sinev, hep-ph/0310246.